First 3D modeling of tungsten erosion and migration in WEST discharges adopting a toroidally non-symmetric wall geometry

S. Di Genova, G. Ciraolo, A. Gallo, J. Romazanov, N. Fedorczak, H. Bufferand, P. Tamain, N. Rivals, Y. Marandet, S. Brezinsek, et al.

▶ **To cite this version:**

S. Di Genova, G. Ciraolo, A. Gallo, J. Romazanov, N. Fedorczak, et al.. First 3D modeling of tungsten erosion and migration in WEST discharges adopting a toroidally non-symmetric wall geometry. Nuclear Materials and Energy, 2023, 34, pp.101340. 10.1016/j.nme.2022.101340 . hal-03988791

HAL Id: hal-03988791
https://hal.science/hal-03988791

Submitted on 14 Feb 2023

HAL is a multi-disciplinary open access archive for the deposit and dissemination of scientific research documents, whether they are published or not. The documents may come from teaching and research institutions in France or abroad, or from public or private research centers.

L'archive ouverte pluridisciplinaire **HAL**, est destinée au dépôt et à la diffusion de documents scientifiques de niveau recherche, publiés ou non, émanant des établissements d'enseignement et de recherche français ou étrangers, des laboratoires publics ou privés.

First 3D modeling of tungsten erosion and migration in WEST discharges adopting a toroidally non-symmetric wall geometry

S. Di Genova [1], G. Ciraolo[2], A. Gallo[2], J. Romazanov[3], N. Fedorczak[2], H. Bufferand[2], P. Tamain[2], N. Rivals[2], Y. Marandet[4], S. Brezinsek[3], E. Serre[1] and the WEST team[5]

[1]M2P2, Aix-Marseille Univ, CNRS, Centrale Marseille, 13013 Marseille,France
[2]IRFM, CEA-Cadarache, 13108 Saint-Paul-lez-Durance, France
[3]IEK-4, Forschungszentrum Jülich, 52425 Jülich , Germany
[4]PIIM, Aix-Marseille Univ, CNRS, 13013 Marseille, France
[5]http://irfm.cea.fr/en/west/WESTteam/

Abstract

Numerical analyses are a key tool to investigate tungsten (W) sources and contamination in W Environment steady-state tokamak (WEST) plasma discharges. Modelling activity was performed in order to study W erosion and migration at WEST plasma-facing components (PFCs), using for the first time a toroidally asymmetric wall geometry provided by toroidally localized objects representing WEST outer limiter or antennae. 3D non-axisymmetric SOLEDGE transport simulations were performed with simplifying assumptions (pure Deuterium plasma, fluid model for neutrals) to reproduce WEST boundary plasma, and used as background for ERO2.0 simulations modelling W erosion, re-deposition, and migration. On the sides of the toroidally localized limiters/antennae, two thin W stripes were considered in order to model WEST W antennae protections. Simulations suggest antennae protections contribution to dominate W contamination in the considered simulations settings, highlighting the need of further analyses with different configurations using this kind of tools.

1 Introduction

The capability of studying heavy elements erosion and migration in tokamaks represents an important task to the interpretation of current and next generation of fusion experiments. Tungsten (W) is considered to be the most suitable material to cover walls and interface plasma in future reactors, and it has being widely tested in tokamaks such as ASDEX [1] and JET-ILW [2]. Some of the Tungsten Environment Steady-state Tokamak (WEST) [3] main goals are to study the feasibility of using W in steady operations and test the divertor monoblocks that will be adopted for ITER. WEST operations are largely influenced by W erosion and migration to the confined plasma, as it is the bulk material for the divertor monoblocks and the coating material for all the Plasma Facing Components (PFCs), some of which are toroidally localized objects, as shwon in figure 1a. Among those toroidally localized PFCs, there are some components whose surface is usually located close to the hot confined plasma, as they are acting as limiters. WEST limiters (as the outboard limiter and the inner bumpers in the discharges start-up, or the radio frequency (RF) antennae protections during the discharges) are strongly eroded [4] and suspected to have a key role in influencing WEST core W content.
In previous contributions, numerical modelling activities was performed in order to study W erosion and migration at WEST PFCs [5] under the working assumption of axisymmetric wall geometry. In this work we first introduce numerical analyses of W erosion and migration in WEST using 3D simulations which include an asymmetric wall geometry composed of both axisymmetric PFCs and toridally localizzed objects, as shwon in figure 1b. We here describe the example of a possible set-up for SOLEDGE [6] and ERO2.0 [7] simulations followed by the discussion of the resulting outputs.

2 Model wall geometry

The model wall geometry evolved from an axisymmetric one, the old axisymmetric wall had a single wide toroidal outer limiter (i.e. an axisymmetric toroidal ring) as shown in figure 2. As the limiter surface was way greater than the surface of interaction of WEST limiters with plasma, the outboard limiter was retracted of an arbitrary distance to avoid overestimating plasma recycling and W erosion as described in [8]. Due to its distance from the main separatrix (roughly 20 cm), the limiter contribution to the overall core W content in simulations was often negligible [5]. Passing to a new wall geometry with toroidally localized objects was possible thanks to

new SOLEDGE developments allowing 3D asymmetric simulations [9]. The new wall had four toroidally localized limiters, that were considered suitable to model antennae as well. The four limiters/antennae were located 90° from the next ones, with their distance from the separatrix of the considered magnetic configuration being about 1.5 cm. This is quite a small distance, even if it is not unusual in WEST experiments to have distances between separatrix and the first object in the Low Field Side (LFS) smaller than 2cm, with average values being around 3 cm [4], so the distance considered here can be seen as a lower limit.
The wall PFCs were divided in three different types as shown in figure 3: The Axisymmetric ones were always considered W sources. The ones consisting of the body of the limiters/antennae (10° wide each) were never considered W sources, as they were aimed to represent the antennae central components made of middle Z elements, as silver (Ag) and copper (Cu).Finally, the ones consisting of the sides of limiters/antennae (3.5° each) were not considered W sources in a first simulation and then used as W source in a second run to study their impact on the overall W core content. The purpose of those PFCs was to model the W antennae protections present in WEST, therefore they will be referred now on as the antennae protections.
For technological limitations that will be discussed in the next session, in this model the wall surfaces were either parallel or orthogonal to the toroidal direction, so they were intersected by the toroidal component of the magnetic field with an azimuthal angle that could be either 0°, as the axisymmetric components, or 90°, as the side surfaces of the limiters/antennae (the presence of the poloidal component of the magnetic field prevents having null intersections between the field and the wall). For this reason, the actual curved "bumping" shape of the antennae protections could not be here reproduced, with the magnetic field intersecting the sides of the antennae protections nearly orthogonally. The effect of this idealisation is expected to be the overestimation of W erosion rate at antennae protections, and the underestimation of prompt re-deposition of W particles coming from their surface, as W Larmor gyration plane would be nearly parallel to the erosion surface.

3 Modelling boundary plasma

Boundary plasma was modelled through SOLEDGE [6, 9]. SOLEDGE is capable of solving fluid equations for multiple species from the edge plasma up to the first wall in complex geometries. SOLEDGE adopts flux-surface aligned structured mesh in which quadrangles in the poloidal plane are ex-

truded in the toroidal direction. The wall geometry is imposed through boundary conditions immersed inside the mesh, so the wall surfaces can't be tilted in respect to the toroidal direction as explained in the previous section.

The simulation here described was in pure deuterium (D), turbulent phenomena were accounted just on "large" tokamak scales through diffusive processes (i.e. a transport simulation) adopting mean-field transport coefficients for particle cross-field diffusion $D_\perp$ and viscosity $\nu_\perp$ such as : $D_\perp = \nu_\perp = 0.3$ m^2/s and cross-field heat conductivity for ions $\chi^{\mathrm{i}}_\perp$ and electrons $\chi^{\mathrm{e}}_\perp$ such as: $\chi^{\mathrm{i}}_\perp = \chi^{\mathrm{e}}_\perp = 1$ m^2/s. Drifts were not included in the runs. Neutrals physics were handled with a single diffusive fluid model in SOLEDGDE itself, as the coupling between SOLEDGE and EIRENE, accomplished in 2D simulations [6], is still in development for 3D simulations with toroidally asymmetric walls.

The total power entering in the scrape-off layer P_{SOL} was set to 1MW, the electron density n_{e} at the core-edge interface (the simulation inner boundary) was set to 5×10^{19} m^{-3}, and a neutral gas injection rate (or puff) of 7×10^{20} s^{-1} was located in the private flux region, the recycling coefficient was set to be on whole wall surface equal to 97% (lower than usual values used for W to account the pumps effect).

The simulation was run with symmetry in respect to a quarter of torus, the quarter of torus toroidal discretization consisted of 32 sectors of roughly 0.05 rad each (2.81°).

Representative figures of the 3D simulation can be found in figures 4 and 5. Figure 5 represents the parallel velcoity field in a poloidal corss section of the torus, at LFS, Plasma flow goes axysimmetrially in the magnetic field direction at the top of the machine and in the opposite direction at the bottom. The presence of toroidally localized objects breaks the axisymmetry with plasma flowing in opposite directions at the two sides of the antennae. Trivially, this effect can't be reproduced in 2D simulations. Despite the simplified model, SOLEDGE results were realistically inside WEST operational space in L-mode, with values that could be the ones of a typical WEST discharge: figure 6 and 7 show density and temperature at outer midplane and divertor targets rispectivelly in the simulation, at a toroidal angle halfway between two antennae: n_{e} at the outer midplane separatrix was 2.5×10^{19} [m^{-3}], going up to 3.4×10^{19} [m^{-3}] at the outer target due to recycling at divertor plates. T_{e} went from 50 [eV] at the separatrix down to 30 [eV] at the outer target, as the plasma was in conduction limited regime. T_{i} at antennae major radius was roughly 50 eV and its variation along the toroidal angle was negligible, likewise, T_{e} modulation in the toroidal direction was also insignificant. On the other hand, plasma flux strongly varied along the toroidal field, as

plasma went repeatedly from stagnant to sound speed along the magnetic lines as a results of Bohm condition at the antennae surfaces. In figure 8 plasma parallel velocity field at a major radius greater than the antennae one is shown, the field at the two sides of each antenna is not symmetrical, as the poloidal magnetic topology in the upper and the lower part of the machine is not identical. Density slightly modulates in the toroidal direction as a result of plasma recycling at antennae surface and the fact that flux along the magnetic lines roughly conserved itself. In figure 9 the relative midplane toroidal modulation at antenna major radius is shown for n_e, T_e, T_i, and $v_\parallel$. The relative midplane toroidal modulation of a quantity A at a certain value φ of the toroidal angle is defined as $\bar{A}(\varphi) = (A(\varphi) - < A >_{2\pi})/\mathrm{Max}(A)_{2\pi}$, with the toroidal average $< ... >_{2\pi}$ and the maximum on the toroidal angle $\mathrm{Max}(...)_{2\pi}$ reported for each physical quantity in table 1.

4 Modelling W erosion and migration

W erosion and migration was modelled through ERO2.0 [7]. ERO2.0 is a code dedicated to Monte Carlo impurity tracking and surface erosion or deposition computation. The geometry described in section 2 was adopted as wall, i.e. the surface from which W is eroded and the boundary to which it deposits, SOLEDGE results described in section 3 were used as plasma background for ERO2.0 runs, In this way SOLEDGE and ERO2.0 simulations geometries are completely compatible. Actually, ERO2.0 is capable to handle any wall geometry, so a more realistic geometry of the antennae protections could be used, extrapolating SOLEDGE results outside its wall. However, in this work it was preferred to keep consistency between SOLEDGE and ERO2.0 simulations.

It is well known how W sputtered by D is supposed to be negligible compared to sputtering by light impurities in L-mode discharges [10]. Uniform concentration values of oxygen (O) of 3% was set in ERO2.0 simulations as a proxy of the different light impurities usually found in WEST such as nitrogen (N), borum (B), and carbon (C). O ionisation states abundance (i.e. relative concentration) from 1+ to 8+ was set to be equal to the values found at the divertor of 2D SOLEDGE simulations in WEST geometry, with inputs not too far from the ones described here, in which O distribution was self-consistently computed [11]. Thompson distribution [12] was used for the energy of the sputtered particles, while a butterfly-like distribution [12] was used for the azimuthal angle of sputtered W. Turbulent transport was modelled with random cross-field displacements at each particles motion time step Δt equal to $\sqrt{4D_\perp \Delta t}$, with the diffusion coefficient $D_\perp$ considered equal

to the value used in SOLEDGE. Inside the sheath, the electrostatic potential ϕ followed the Borodkina model [13] and n_e dropped, as well known [14], proportionally to the Boltzmann factor $\exp(e\phi/T_e)$, where e is the electron charge. The model collisional forces included both kinetic formulae for friction forces F_0 and thermal forces $F_{\nabla T}$ as widely described in literature [15,16]. Contamination from W self-sputtering was not included to keep the analyses simple and linear.
As explained in section 2, simulations were repeated with and without considering the antennae protections as W sources, figure 10 show W density maps from the two cases results: in the case without antennae protections source, the main contribution to core (i.e. the part of confined plasma included in simulations) W content was given by the top of the machine, while in the opposite case W coming from the antennae protections dominate the core. The global picture of the density map changes between the two cases, with the edge W level being roughly one order of magnitude higher in the case including the antennae protections source. As self-sputtering was not included in simulations, PFCs impact on W content is linear and the difference of density between simulations is purely caused by plasma erosion of the antennae protections.Table 2 reports the values of the total number of W particles found inside the separatrix coming from the antennae protections and from the rest of the PFCs. likewise, the erosion rate of the two groups of PFCs is also written in the table. In percentage, 85% of the erosion rate in caused by the plasma interaction with the axisymmetric PFCS (lower divertor, upper divertor, baffle, tokamak ceiling), but 90% of W particles found in the separatrix comes the antennae protections. This result may overestimate the actual impact of the antennae protections in experiments, as the distance from the separatrix is particularly small (even if not unrealistic), and those PFCs are not tilted in respect to toroidal component of the magnetic field. Nevertheless, the impact of the toroidal localized objects seems to be quite relevant.

5 Conclusions

WEST boundary plasma, wall erosion, and W migration was modelled in a toroidally asymmetric wall geometry including toroidaly localized objects. Pure D SOLEDGE 3D simulations were carried out to reproduce plasma main species (D and e) conditions, using a simple fluid model for neutrals and diffusive processes as a proxy for turbulent transport. ERO2.0 simulations were run to model W erosion and migration, adopting a uniform concentration of O of 3% to model W sputtering by light impurities. Simulations were

repeated with and without considering W erosion at antennae protections. The big impact of the antennae protection on the overall W content inside the separatrix in the considered configuration suggests that toroidally localized objects modelling could be a key tool for the interpretations of boundary phenomena and impurity physics in experiments, encouraging modelling activity adopting 3D toroidally asymmetric walls, improving the consistency with the experiment geometry and scanning toroidally localized objects distance from the separatrix, as well as analyse different plasma regimes and scenarios.

Aknowldgment

This work has been carried out within the framework of the EUROfusion Consortium and has received funding from the Euratom research and training programme 2014-2018 and 2019-2020 under grant agreement No 633053. The views and opinions expressed herein do not necessarily reflect those of the European Commission.

Figures

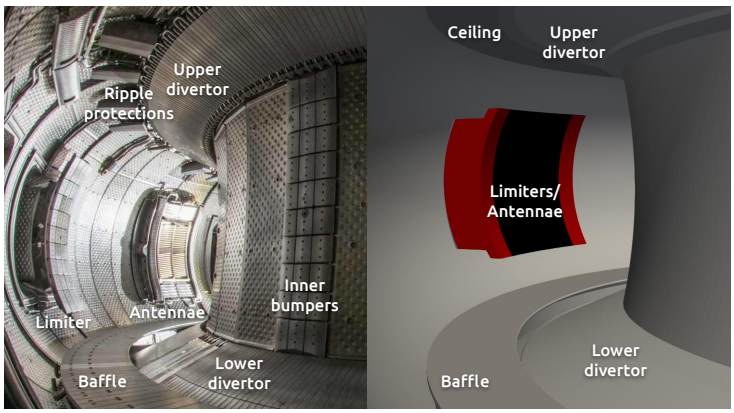

(a) (b)

Figure 1: a) WEST PFCs, completely made by bulk W, or coated with W (up to C4 campaign, 2019). Among them, some are toroidally localized objects (Inner bumpers, RF antennae, outboard limiter). b) New simplified WEST wall model, composed by axysimmetric surfaces and toroidally localized PFCs.

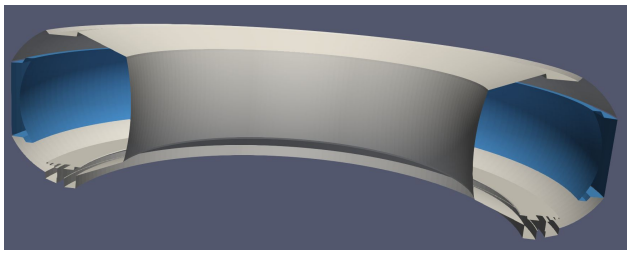

Figure 2: Previous WEST axisymmetric wall model, adopted in [5, 11]. The axisymmetric limiter/antenna can be seen (blue component in figure). To avoid overestimating recycling and erosion, due to the large surface of the limiter, this component was located at an arbitrary position far from the core.

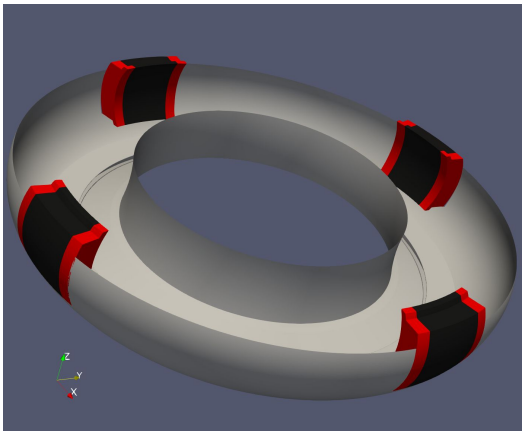

Figure 3: New WEST asymmetric wall model, including toroidally localized PFCs that can be seen as outboard limiters or antennae. The axysimmetric PFCs in figure (in grey) were always considered W sources, the black PFCs in figure were never considered W sources (modelling WEST components made by middle Z materials). Finally, the red PFCs W source was switched on and off to study its impact on W confined plasma contain, as they represent WEST W antennae protections.

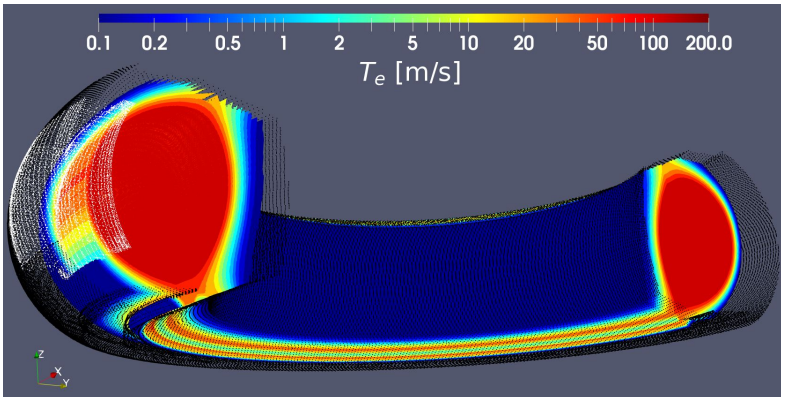

Figure 4: T_e iso-surfaces on half of a torus, including only the surface with $T_e > 0.1$ [eV]. Black dots represent the axysimmetric part of the wall, white dots represent the toroidally localized objects. T_e at antennae surface is similar to the one at the divertor plates (visible at the bottom of the torus).

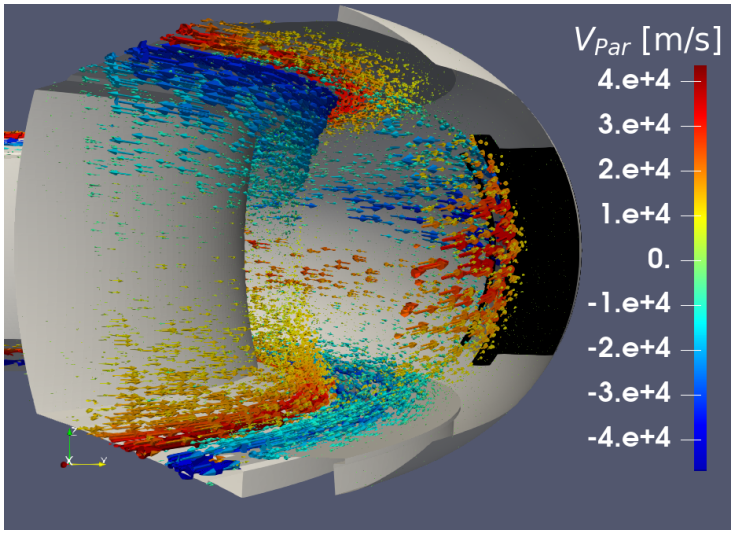

Figure 5: Plasma parallel velocity field seen from a torus poloidal cross section. The magnetic field enters in the figure plane, going in counterclockwise direction seeing the tokamak from the top. Red arrows go in the same direction of the magnetic field, blue arrows go in the counter direction.

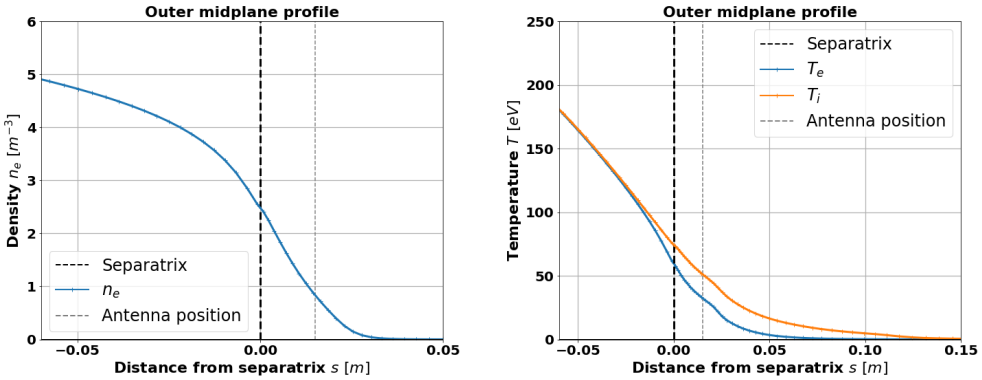

(a) (b)

Figure 6: SOLEDGE results midplane plots at a toroidal angle equidistant from 2 antennae for a) n_e, and b) T_i and T_e.

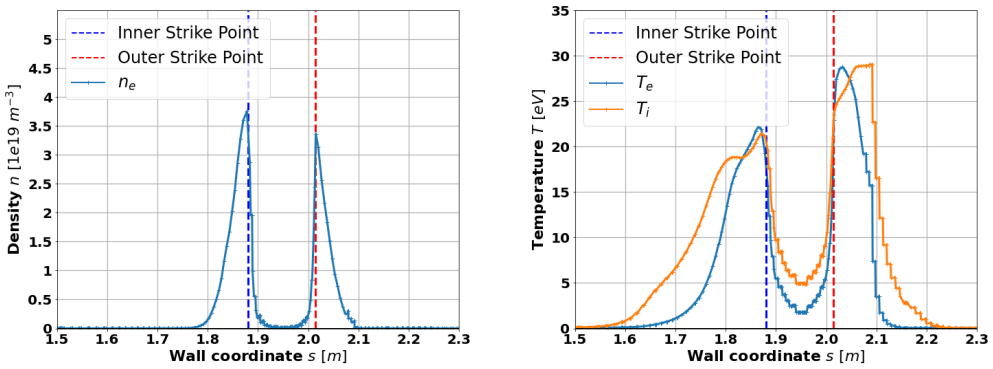

(a) (b)

Figure 7: SOLEDGE results divertor targets plots at a toroidal angle equidistant from 2 antennae for a) n_e, and b) T_i and T_e.

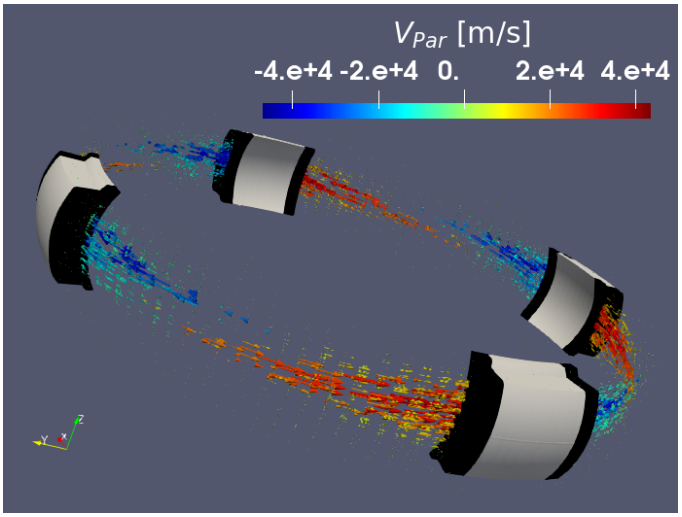

Figure 8: Plasma parallel velocity field at a major radius greater than the antennae one. Plasma parallel flow is slightly tilted in respect to the toroidal direction due to the poloidal component of the magnetic field.

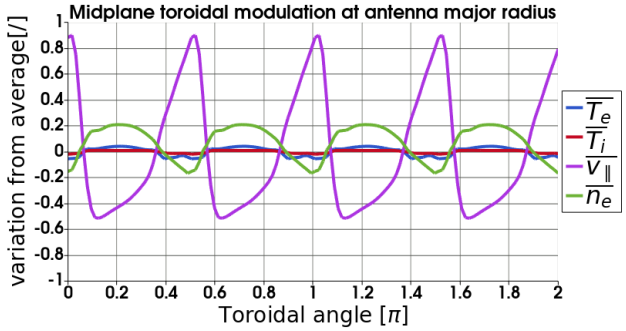

Figure 9: Relative midplane toroidal modulation of plasma physical quantities as defined in section 2. T_i and T_e varies along the toroidal direction from the average less than 0.05 times the max assumed value. The modulations are more important for n_e and $v_\parallel$.

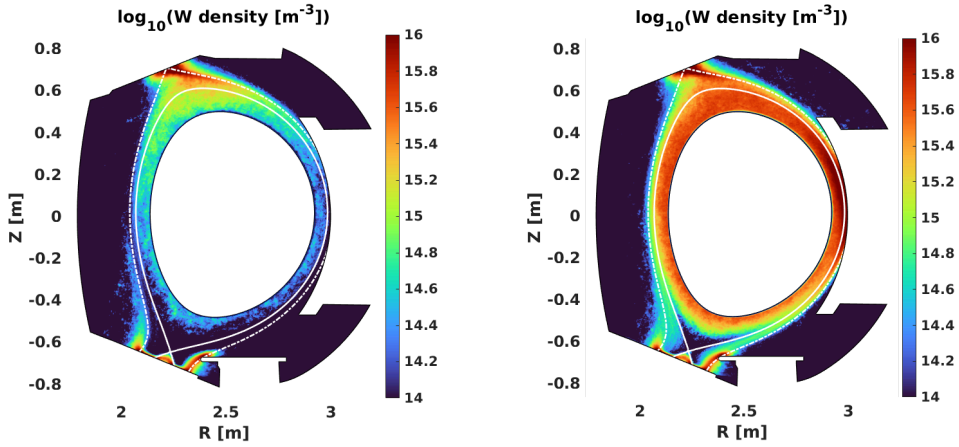

(a) (b)

Figure 10: W density maps: a) without considering antennae protections W erosion, and b) considering it.

Tables

	$<>_{2\pi}$	$\mathrm{Max}()_{2\pi}$
T_e [eV]	31.4	31.8
T_i [eV]	55.2	55.8
n_e [10^{18} m^{-3}]	6.0	7.0
$v_\parallel$ [10^4 m s^{-1}]	0.2	2.0

Table 1: Average and maximum values assumed by physical quantities along the toroidal angle φ at the midplane at antenna major radius.

	Antennae protections	Rest of PFCs
Erosion rate [s^{-1}]	3.27×10^{19}	2.54×10^{20}
W ions inside separatrix [/]	9.00×10^{16}	9.95×10^{15}

Table 2: Values comparison of ERO2.0 results. Antennae protections contribute 90% of the overall W confined plasma content, but 85% of the erosion comes from the rest of the PFCs

References

[1] A. Kallenbach et al. Non-boronized compared with boronized operation of ASDEX upgrade with full-tungsten plasma facing components. *Nuclear Fusion*, 49(4):045007, mar 2009.

[2] S. Brezinsek et al. Plasma-surface interaction in the Be/W/ environment: Conclusions drawn from the JET-ILW for ITER. *Journal of Nuclear Materials*, 463:11–21, 2015. PLASMA-SURFACE INTERACTIONS 21.

[3] J. Bucalossi et al. The WEST project: Testing ITER divertor high heat flux component technology in a steady state tokamak environment. *Fusion Engineering and Design*, 89(7):907–912, 2014. Proceedings of the 11th International Symposium on Fusion Nuclear Technology-11 (ISFNT-11) Barcelona, Spain, 15-20 September, 2013.

[4] G. Urbanczyk et al. RF wave coupling, plasma heating and characterization of induced plasma-material interactions in WEST L-mode discharges. *Nucl. Fusion*, 61, 2021.

[5] S. Di Genova et al. Modelling of tungsten contamination and screening in WEST plasma discharges. *Nuclear Fusion*, 61(10), 2021.

[6] H. Bufferand et al. Numerical modelling for divertor design of the WEST device with a focus on plasma–wall interactions. *Nuclear Fusion*, 55(5):053025, apr 2015.

[7] J. Romazanov et al. Beryllium global erosion and deposition at JET-ILW simulated with ERO2.0. *Nuclear Materials and Energy*, 18:331–338, 2019.

[8] A. Gallo et al. First efforts in numerical modeling of tungsten migration in WEST with SolEdge2D-EIRENE and ERO2.0. *Physica Scripta*, T171, jan 2020.

[9] H. Bufferand et al. Three-dimensional modelling of edge multi-component plasma taking into account realistic wall geometry. *Nuclear Materials and Energy*, 18:82–86, 2019.

[10] A. Huber et al. Understanding tungsten erosion during inter/intra-ELM periods in he-dominated JET-ILW plasmas. *Physica Scripta*, 96(12), 2021.

[11] A. Gallo et al. Interpretative transport modeling of the WEST boundary plasma: main plasma and light impurities. *Nuclear Fusion*, 60(12), nov 2020.

[12] A. Eksaeva et al. ERO modelling of tungsten erosion in the linear plasma device PSI-2. *Nuclear Materials and Energy*, 12, 03 2017.

[13] I. Borodkina et al. Surface biasing influence on the physical sputtering in fusion devices. In *Journal of Physics: Conference Series*, volume 748, page 012002. IOP Publishing, 2016.

[14] P.C. Stangeby. *The Plasma Boundary of Magnetic Fusion Devices*. Series in Plasma Physics and Fluid Dynamics. Taylor & Francis, 2000.

[15] D. Reiser et al. Improved kinetic test particle model for impurity transport in tokamaks. *Nuclear fusion*, 38(2):165, 1998.

[16] Y. Homma et al. Numerical modeling of thermal force in a plasma for test-ion transport simulation based on monte carlo binary collision model. *Journal of Computational Physics*, 231(8):3211–3227, 2012.